ADVANCES IN ATMOSPHERIC SCIENCES, VOL. 22, NO. 3, 2005, 451–462

On the Mechanism of the Seasonal Variability of SST in the Tropical Indian Ocean

HU Ruijin*[1] (胡瑞金), LIU Qinyu[1] (刘秦玉), MENG Xiangfeng[1] (孟祥凤), and J. Stuart GODFREY[2]

[1] *Physical Oceanography Laboratory and Ocean-Atmosphere Interaction and Climate Laboratory, Ocean University of China, Qingdao* 266003

[2] *CSIRO, Division of Marine Research, GPO Box* 1538, *Hobart, Tasmania, Australia*

(Received 29 January 2004; revised 1 November 2004)

ABSTRACT

A general form of an equation that "explicitly" diagnoses SST change is derived. All other equations in wide use are its special case. Combining with the data from an ocean general circulation model (MOM2) with an integration of 10 years (1987–1996), the relative importances of various processes that determine seasonal variations of SST in the tropical Indian Ocean are compared mainly for January, April, July and October. The main results are as follows. (1) The net surface heat flux is the most important factor affecting SST over the Arabian Sea, the Bay of Bengal and the region south of the equator in January; in April, its influence covers almost the whole region studied; whereas in July and October, this term shows significance only in the regions south of 10°S and north of the equator, respectively. (2) The horizontal advection dominates in the East African-Arabian coast and the region around the equator in January and July; in October, the region is located south of 10°S. (3) The entrainment is significant only in a narrow band centered on 10°S in April and the coastal region around the Arabian Sea and the equator in July. (4) As for SST, it decreases in January and July but increases in April and October in the Arabian Sea and the Bay of Bengal, showing a (asymmetrical) semiannual variability; by contrast, the SST in the region south of the equator has an annual variability, decreasing in April and July and increasing in October and January.

Key words: new equation, SST, seasonal variation, mechanism, tropical Indian Ocean

1. Introduction

Many researchers have pointed out that the sea surface temperature (SST) in the tropical Indian Ocean affects not only the rainfall in India (Shukla and Mooley, 1987) and Australia (Nichols, 1985), but also the East Asian monsoon (Xiao and Yan, 2001), the northwestern Pacific subtropical high (Wu et al., 2000) and the summer rainfall in China (Chen, 1991). So more and more studies have focused on the Indian Ocean. Recently, the discovery of the Indian Ocean dipole event (Saji et al., 1999), which shows that the Indian Ocean can develop an independent ENSO-like variability mechanism (Webster et al., 1999), gives rise to new interests in this region (Murtugudde and Busalacchi, 1999; Li and Mu, 2001).

SST change may be driven directly from above, by changes in the atmospheric quantities such as near-surface wind speed, air temperature and humidity, solar radiation and cloud cover. The second kind of SST change is driven from below, by horizontal or vertical currents in the ocean or by vertical mixing. To study the mechanism of SST variation, it is useful to determine the relative importance of different processes in the change of SST, based on an equation that is intimately related to SST.

The equation for the heat budget of the upper ocean is one such a kind of equation. Similar to studies on SST dynamics in the Pacific (e.g., McPhaden and Hayes, 1991; Feng et al., 1998; Qiu, 2000), many authors focus on the heat budget and SST in the tropical Indian Ocean. For example, McPhaden (1982) pointed out that 80% of the variation of the mixed layer can be accounted for by the surface heat flux, based on the records near Gan Island of the equatorial central Indian Ocean; Shetye (1986) studied the annual cycle

*E-mail: huruijin@ouc.edu.cn

of SST within a 2° band between the Somali coast and southwest India and compared the relative importance of surface heat flux, horizontal advection and vertical advection in determining SST. These studies out that all contributions are important in summer, but only the local effect is large for the other seasons; Qu et al. (1994) found that the surface heat flux is dominant in the variation of SST off northwest Australia, but that the ocean also plays a role. These studies certainly shed light on the physics of SST variation, but they are limited to small regions in the tropical Indian Ocean and the results are region means or at a single point. Although Rao and Sivakumar (2000) investigated the heat budget and SST for the whole tropical Indian Ocean, based on observations, the equation they used is an approximate one. The same problem also exists in the study of Behera et al. (2000), who discussed the evolution of SST in the tropical Indian Ocean using a two-and-a-half layer reduced gravity model (McCreary et al., 1993). In fact, all heat budget equations used to "explicitly" diagnose SST change need to be extended. Besides this, the OGCM studies of the dynamics of SST for the whole tropical Indian Ocean are very few in number.

In this paper, we focus on the study of the mechanism that determines the seasonal variation of SST in the whole tropical Indian Ocean, based on an equation that is an extension of others and is derived by the authors of this paper, using the dataset of a 10-year integration from an ocean general circulation model (MOM2).

The structure of this paper is as follows. Section 2 gives the outline of the details of the model and its assessment. In section 3, the derivation of the equation that is used to diagnose SST change is represented. Section 4 shows the evaluation of this equation and the analysis of the relative roles of various processes in the seasonal variation of SST for the whole tropical Indian Ocean. The paper is ended with a summary.

2. The model and its assessment

2.1 *Model details*

The model is a global ocean circulation model based on the Modular Ocean Model version 2 (MOM2) version (Pacanowski, 1995; Godfrey et al., 2003, manuscript submitted to *J. Geophys. Res*). The zonal resolution is 2°, the meridional resolution is 0.5° within 10°S–10°N, increasing poleward with a 5.85° grid spacing near the poles. The vertical is divided into 25 levels with a maximum depth of 5000 m and 12 levels in the upper 185 m. The integration time step is 900 s.

The wind stress is from the FSU wind atlas (Legler et al., 1989; Stricherz et al., 1992), with $C_d = 0.0015$, blended with Hellerman and Rosenstein (1983) wind stresses poleward of 30°N/S. The heat flux is parameterized using ISCCP net solar shortwave radiation plus flux correction (Schiller et al., 1998). The fresh water flux is restored to Levitus et al. (1994) data. The horizontal viscosity and diffusivity are 4000 $m^2\ s^{-1}$, and the vertical viscosity and diffusivity are determined by the Chen scheme (Chen et al., 1994; Godfrey and Schiller 1997). In the Indonesian archipelago region, the vertical diffusion and viscosity are increased to simulate tidal mixing there (Ffield and Gordon, 1992). Salinity is relaxed to observed values near the mouth of the Red Sea. Water transparency varies with position according to Simonot and Letreut (1986).

The model was first spun up for 10 years with mean seasonal wind stresses and speeds, humidity fraction and shortwave radiation, plus strong relaxation to observed SSTs. Seasonal flux corrections were calculated, and subsequent runs started from conditions at the end of this spinup run, using meteorological forcing for 1985–1996, with flux corrections applied.

2.2 *Model assessment*

It is indispensable to check whether the model gives a reasonable simulation of the real Indian Ocean before doing further analysis. A comprehensive study for comparing the outputs of this model with observations was made by Hu (2003), so here only the comparison of SST is given (Figs. 1–3). As shown in Fig. 1, the annual mean SST in the tropical Indian Ocean from the model is quite close to that from Simple Ocean Data Assimilation (SODA) data (Carton et al., 2000). This is also true for the seasonal variation of SST (Figs. 2 and 3). Similar results can be obtained if we compare the variance of SST or the seasonal cycle of the area mean SST (north of 20°S in the Indian Ocean) between these two datasets (figures not shown). This means the model reproduces SST very well in this region. This model also gives realistic simulations of mixed layer depth, ocean current, etc. (Hu, 2003), despite its relatively low resolution (figures not shown). For example, the model's 16 Sv (1 Sv=$10^6\ m^3\ s^{-1}$) value for the annual mean volume transport of the Indonesian throughflow (ITF) is within the reasonable range (Godfrey, 1996). So the results from the model are credible. The output of this model includes sea temperature, salinity, ocean current, horizontal wind stresses and net surface heat flux, etc. It is worth mentioning that the net surface heat flux is the one with the flux correction added. These data (monthly, from 1987–1996) will be used to compare the relative importance of various processes

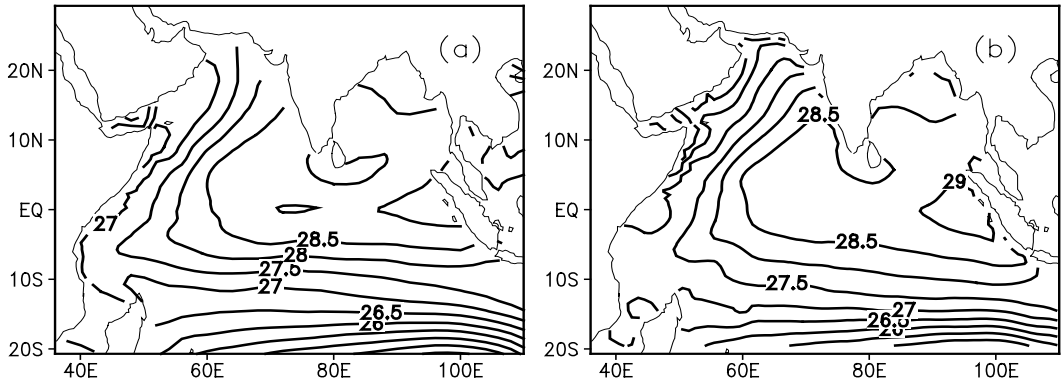

Fig. 1. Annual mean SST for the tropical Indian Ocean: (a) from the model, (b) from SODA. Contour interval: 0.5°C.

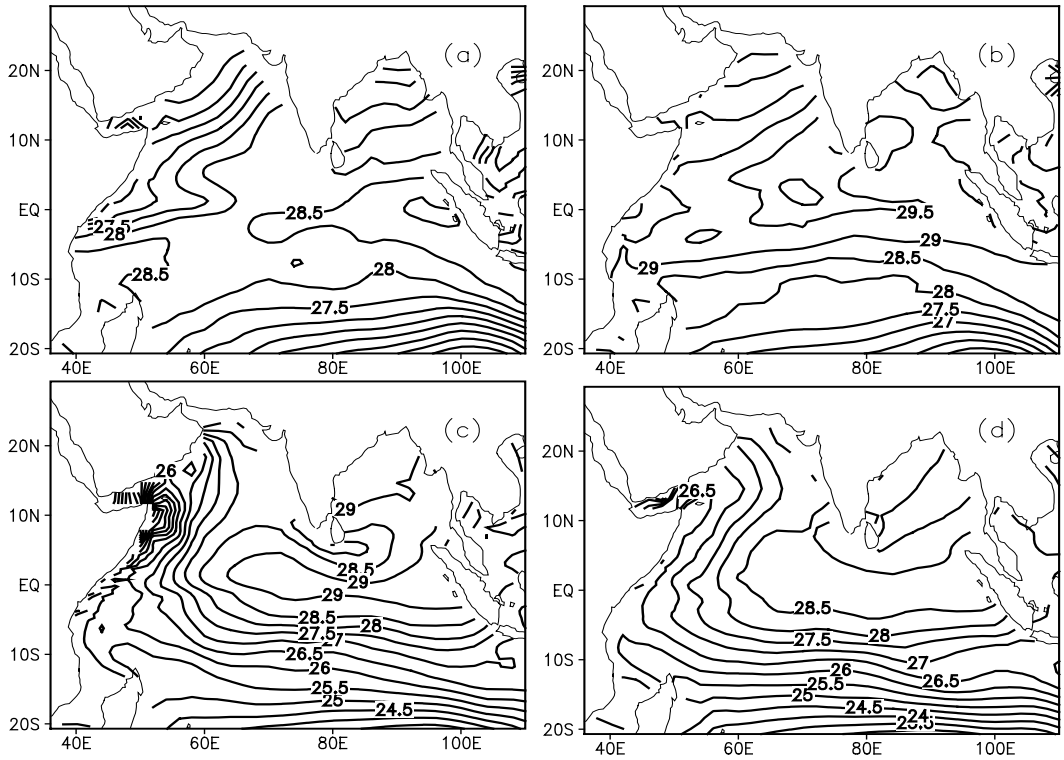

Fig. 2. Seasonal variation of SST in model for the tropical Indian Ocean. (a) January, (b) April, (c) July, (d) October. Contour interval: 0.5°C.

that influence the seasonal variation of SST in the tropical Indian Ocean, combined with a new equation that will be described in the next section.

3. The equation

Omitting horizontal diffusivity, the thermodynamic equation can be written as

$$\frac{\partial T}{\partial t}+\boldsymbol{V}\cdot\nabla T+w\frac{\partial T}{\partial Z}=\frac{1}{\rho c_p}\frac{\partial Q}{\partial z}+\frac{\partial}{\partial z}\left(K\frac{\partial T}{\partial z}\right)\ , \quad (1)$$

where T is the sea temperature, $\boldsymbol{V}$ and w the horizontal and vertical velocity, ρ the density of sea water, c_p the specify heat of sea water, Q the vertical heat flux and K the vertical heat diffusivity coefficient.

Using the continuity equation and integrating from the surface to depth h, we get

$$\int_{-h}^{0}\frac{\partial T}{\partial t}dz+\int_{-h}^{0}\nabla\cdot(\boldsymbol{V}T)dz+\int_{-h}^{0}\frac{\partial}{\partial z}(wT)dz$$
$$=\frac{1}{\rho c_p}\int_{-h}^{0}\frac{\partial Q}{\partial z}dz+\int_{-h}^{0}\frac{\partial}{\partial z}\left(K\frac{\partial T}{\partial z}\right)dz\ . \quad (2)$$

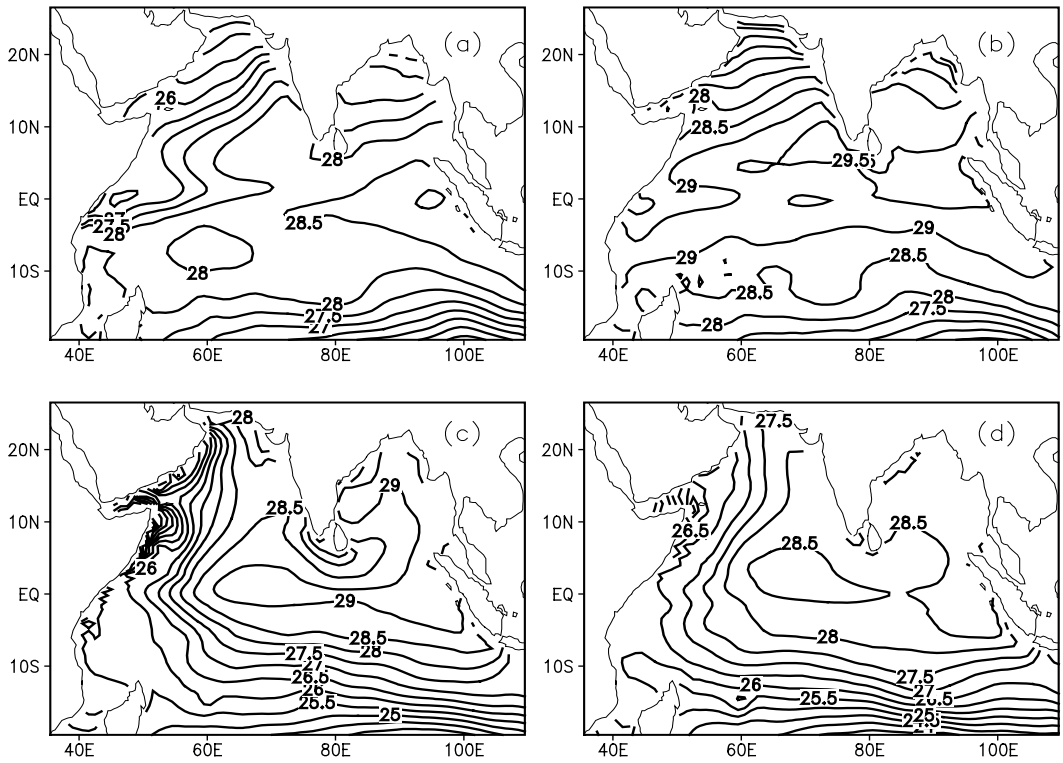

Fig. 3. Same as Fig. 2, but from SODA data. Contour interval: 0.5°C.

We define

$$\overline{T} = \frac{1}{h}\int_{-h}^{0} T dz\ ,\ \ \overline{\boldsymbol{V}} = \frac{1}{h}\int_{-h}^{0} \boldsymbol{V} dz$$

$$T' = T - \overline{T}\ ,\ \ \boldsymbol{V}' = \boldsymbol{V} - \overline{\boldsymbol{V}}\ ,$$

in which $\overline{T}$ and $\overline{\boldsymbol{V}}$ represent the depth (h) averaged temperature and horizontal velocity; T' and $\boldsymbol{V}'$ are the departure of T and $\boldsymbol{V}$ from $\overline{T}$ and $\overline{\boldsymbol{V}}$, respectively.

Ultimately we can get the equation for $\overline{T}$ as follows

$$\frac{\partial \overline{T}}{\partial t} + \overline{\boldsymbol{V}} \cdot \nabla \overline{T} + \nabla \cdot \left(\int_{-h}^{0} \boldsymbol{V}' T' dz \right) + \frac{\overline{T} - T_{-h}}{h} w_{\mathrm{e}} = \frac{Q_0 - Q_{-h}}{\rho c_p h}\ , \qquad (3)$$

where

$$w_{\mathrm{e}} = \frac{\partial h}{\partial t} + \boldsymbol{V}_{-h} \cdot \nabla h + w_{-h}$$

The first term on left side of Eq. (3) represents the rate of change of the depth mean temperature; the second and third terms on the left side are temperature change caused by horizontal advection; the fourth term on the left side side can be called the entrainment term in which w_{e} is the velocity across the surface of depth h; and the first and second terms of the right side of Eq. (3) represent the temperature change caused by net surface heat flux and the heat flux across depth h, respectively. The subscript $-h$ means the value is taken at the depth of h.

Equation (3) is actually the Stevenson-Niiler (1983) equation. It can be used to diagnose which factor is important in the variation of SST, so it is useful in the study of the mechanism of SST change, as long as $\overline{T}$ is a good approximation to SST. This is no problem when depth h is not very large, especially in winter. Of course, to decrease the influence of the error of the second term on the right side of equation (3), h cannot be too small. It should be pointed out that this equation is also suitable for h being constant (in this case, $w_{\mathrm{e}} = w_{-h}$). This equation is widely used. For example, Feng et al. (1998) and Liu et al. (2001) calculated the upper ocean heat balance in the western equatorial Pacific during the westerly wind bursts; and Qiu (2000) diagnosed the interannual variability of the Kuroshio Extension on the wintertime SST anomaly fields, based on an equation that has a slight difference with this one.

However, Eq. (3) is derived under the assumption of no horizontal diffusivity in the thermodynamic equation. If this term is included, the thermodynamic equation will be

$$\frac{\partial T}{\partial t} + \boldsymbol{V} \cdot \nabla T + w \frac{\partial T}{\partial Z} = \frac{1}{\rho c_p} \frac{\partial Q}{\partial z}$$

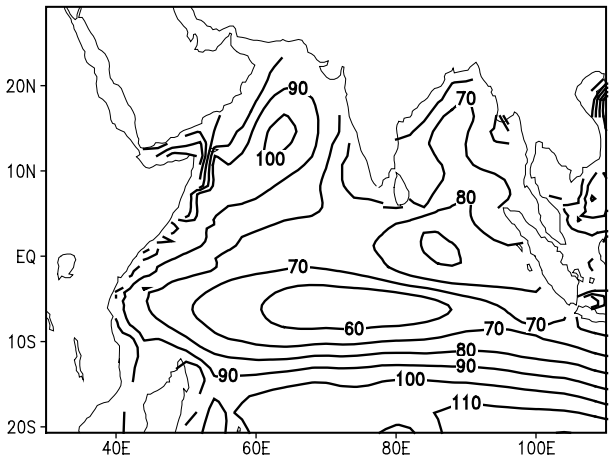

Fig. 4. Annual mean mixed layer depth (from the model) for the tropical Indian Ocean. The depth is defined as values where there is a density difference of 1 kg m^{-3} with the surface. Units: m.

$$+\frac{\partial}{\partial z}\left(K\frac{\partial T}{\partial z}\right)+\nabla\cdot(A_H\nabla T)\,. \qquad (4)$$

Proceeding in a manner similar to above, we obtain (Hu, 2003)

$$\frac{\partial\overline{T}}{\partial t}+\overline{\boldsymbol{V}}\cdot\nabla\overline{T}+\frac{1}{h}\nabla\cdot\left(\int_{-h}^{0}\boldsymbol{V}'T'dz\right)+\frac{\overline{T}-T_{-h}}{h}w_{\rm e}^{*}$$
$$=\frac{Q_0-Q_{-h}}{\rho c_p h}+\nabla\cdot(A_{\rm H}\nabla\overline{T}) \qquad (5)$$

where

$$w_{\rm e}^{*}=\frac{\partial h}{\partial t}+u_{-h}^{*}\frac{\partial h}{\partial x}+v_{-h}^{*}\frac{\partial h}{\partial y}+w_{-h}^{*}\,,$$
$$u_{-h}^{*}=u_{-h}-A_{\rm H}\frac{\partial\ln(\overline{T}-T_{-h})^2}{\partial x}\,,$$
$$v_{-h}^{*}=v_{-h}-A_{\rm H}\frac{\partial\ln(\overline{T}-T_{-h})^2}{\partial y}\,,$$
$$w_{-h}^{*}=w_{-h}-\nabla\cdot(A_{\rm H}\nabla h)\,.$$

The new derived equation (5) is the strict form of the equation for depth-mean temperature ($\overline{T}$) since no assumption was added in the derivation of (5) from the general form of the thermodynamic equation (4). What is more, it is also an "explicit" form of the equation for $\overline{T}$. Comparing equation (5) with (3), we can see that the difference between them is that the $w_{\rm e}$ in (3) is replaced by $w_{\rm e}^{*}$ in (5) and a term is added to the right side of (5). The former is related to the addition of horizontal-diffusion-induced velocity crossing the surface of depth h and the latter is the depth-mean temperature ($\overline{T}$) change caused directly by its horizontal diffusion. Obviously, if the horizontal diffusion coefficient $A_{\rm H}$ is zero, equation (5) will degenerate into (3), a widely used equation in diagnosing SST change (e.g., Feng et al., 1998). If we take some kind of average or decomposition of (5), many new forms of the equation can be obtained.

4. Calculation and analysis

4.1 *Comparison of the two equations*

Before proceeding any further, we need to check whether there is a big difference between Eqs. (5) and (3). To make such a comparison, we first need to determine the depth h for the tropical Indian Ocean. Many methods can be defined (Hu, 2003), as long as the depth mean temperature ($\overline{T}$) over h is a good approximation to SST. In this paper, h is defined as the depth where there is a density difference of 1 kg m^{-3} with the surface (Hu, 2003). For such a definition, the correlation coefficient between $\overline{T}$ and SST is larger than 0.95 (figure not shown), so we will refer to $\overline{T}$ as SST below except when special notice is given. As for horizontal diffusivity $A_{\rm H}$, the model takes the value of 4000 m^2 s^{-1} (Godfrey et al., 2003, manuscript submitted to *J. Geophys. Res.*; Hu, 2003). To show a clear scenario of h, Fig. 4 gives the distribution of its annual mean based on this definition and the model output. The figure shows that the eastern equatorial Indian Ocean and the central Arabian Sea are regions of larger depth, whereas near 5°S, the depth is shallower. These regions are associated with the equatorial westerly (McCreary et al., 1993), local forcing (Rao and Sivakumar, 2000) and Ekman divergence (Schott and McCreary, 2001), respectively.

Figure 5 shows the difference of the fourth term (i.e., entrainment term) on the left side of Eqs. (5) and (3), averaged over 10 years, for the tropical Indian Ocean. It is evident that the big difference is mainly confined to the region of the west boundary of the northern Indian Ocean where the slope of h is large. In absolute value, the maximum is larger than 0.8°C month^{-1}. This means that the SST change caused by crossing a surface h due to horizontal diffusivity cannot be omitted in this region. The magnitude of the third term on the right of Eq. (5) is relatively small (figure not shown).

4.2 *Comparison of different terms for each point using the new Eq. (5)*

It is obvious that many processes such as advection, entrainment, heat flux and diffusion, etc. can lead to SST change in the Indian Ocean. The contributions of each process to such change may be quite different, and such differences may vary with time and space. To investigate the relative importance of various processes, as well as the spatial and temporal differences for such importances, we compare the magnitude of

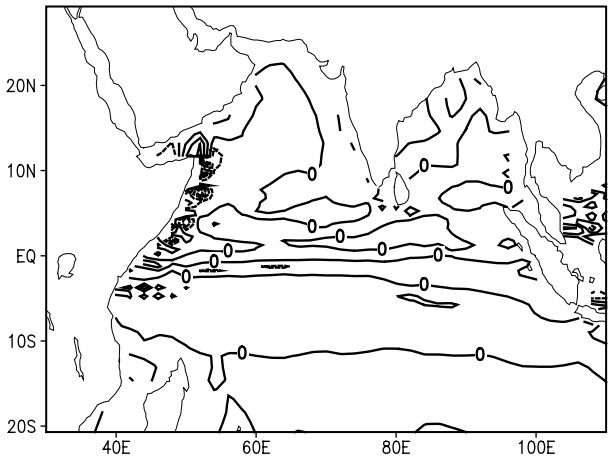

Fig. 5. The difference of the fourth term (i.e., entrainment term) on the left side of Eqs. (5) and (3), averaged over 10 years, for the tropical Indian Ocean. Contour interval: 0.1°C month^{-1}.

each term in Eq. (5).

The method is described as follows. Firstly, we will calculate the seasonal cycle for each term of Eq. (5) in each grid (the second term on the right side, i.e., the Q_{-h} term, is by subtraction); secondly, we take their absolute value (except for the time-varying term of temperature) and compare among them (not including the time-varying term). The term with the maximum (absolute) value is regarded as the most important one that influences the seasonal variation of SST. Such a comparison can be made for each grid, so it is possible to get the spatial distribution of the relative importance of various terms; such a comparison can also be made for each month, so it is also possible to explore the relationships among different months. We do not take the absolute value of the time-varying term and compare it with the others, but instead we give its real seasonal cycle–the purpose is to make it easier for us to analyze the links between this term and the term with maximum (absolute) value. It should be pointed out that such a method is quite rare in the study of dynamics of SST variations, both for the Indian Ocean and other oceans.

Figures 6–9 show the time-varying term of temperature (contours) and the distributions of the term that is the most important (shading) among net surface heat flux, horizontal advection, and entrainment, in the tropical Indian Ocean and for January, April, July and October, respectively. The term across depth h and the term caused directly by horizontal diffusion of $\overline{T}$ (i.e., the second and the third terms on the right side of Eq. (5)) are not shown due to their small values. To include as much information as possible, the real values of net surface heat flux, horizontal advection, and entrainment are also overlaid (contours) on each separate plot. It should be noted that the comparisons among various terms in other months besides the aforementioned four months are also briefly described below.

4.2.1 *For January* (*winter*)

It is shown that in January, the time-varying term (upper left panel of Fig. 6) is negative for most of the Arabian Sea and the Bay of Bengal. This means SST decreases in these regions. The maximum rate of decrease is located on the northern tip of the Arabian Sea with (absolute) value larger than 0.8°C month^{-1}. For other regions of the tropical Indian Ocean, the time-varying term is positive, and the magnitude roughly increases with a latitude with a maximum value larger than 1.0°C month^{-1} near 20°S.

For most of the Arabian Sea and the Bay of Bengal, as well as the region south of the equator, the net surface heat flux dominates the SST change (upper right panel of Fig. 6). For the East African coast and the region of the equator to roughly 10°N, west of 85°E, the horizontal advection is the most important process to influence SST (lower left panel of Fig. 6), which is intimately related to the Somali current. The contribution to SST change from entrainment can be omitted (lower right panel of Fig. 6).

It should be pointed out that the basic patterns are roughly the same for February and December (figures not shown).

4.2.2 *For April* (*spring*)

For April, the time-varying term (upper left panel of Fig. 7) is positive north of the equator (north of 5°S for the region east of 70°E). The contour is oriented southwest-northeast near the East African coast and the Arabian Sea with a maximum value larger than 1.8°C month^{-1} in the northwest Arabian Sea. In the Bay of Bengal, the contour is roughly parallel to the equator with a maximum value larger than 1.2°C month^{-1} in the north of the bay. In the region south of the equator (north of 5°S for the region east of 70°E) the term is negative, and the maximum decreasing rate is about 0.6°C month^{-1} near 20°S between 50°E and 70°E.

Except for a small narrow band centered on 10°S west of 90°E where entrainment is the most important (lower right panel of Fig. 7), and for a small region near the entry of the Indonesian throughflow where the contribution from horizontal advection is largest (lower left panel of Fig. 7), the net surface heat flux dominates the variation of SST in the whole region (upper right panel of Fig. 7). It can be seen, however, that entrainment and horizontal advection also contribute to the distribution of the time varying of SST.

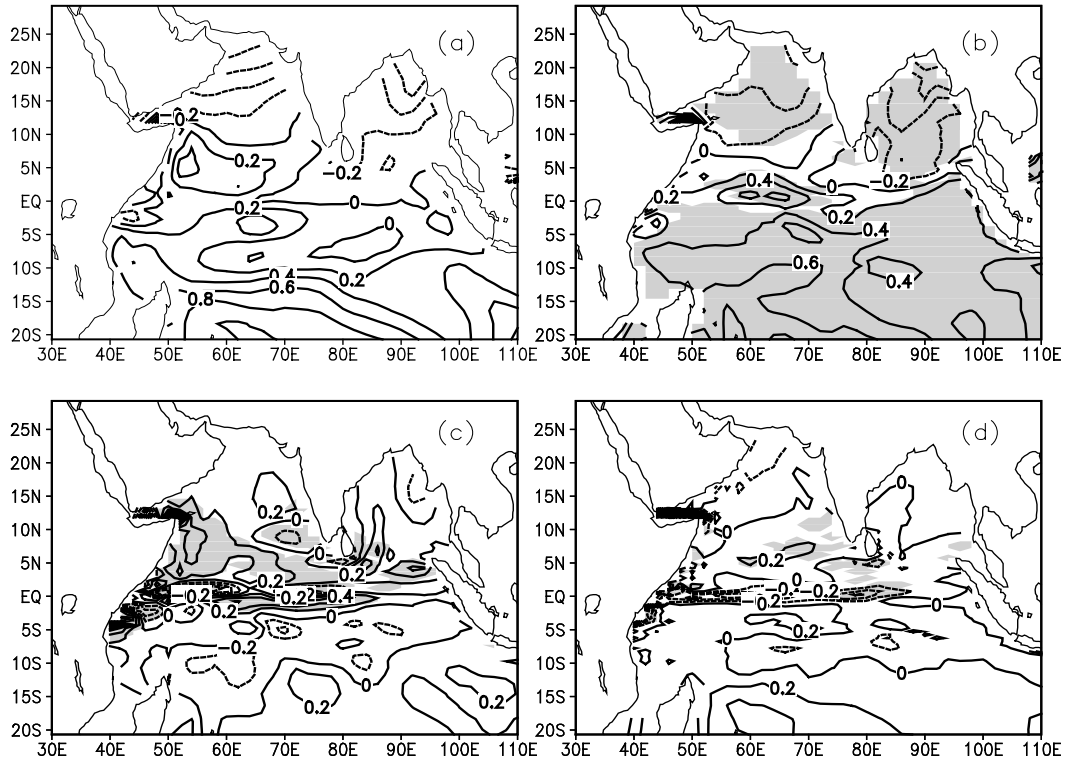

Fig. 6. (a) The magnitude of the time-varying term of temperature (dTdt term), and the distributions of the term that is most important among (b) net surface heat flux (Qnet term), (c) horizontal advection (adv term), and (d) entrainment (entr term), for the tropical Indian Ocean for January. The region where the above term dominates is shaded. The second and the third terms on the right side of equation (5) are not shown due to their small values. To include as much information as possible, the real value of net surface heat flux, horizontal advection, and entrainment are also overlaid (contours) on each respective plot. Contour interval: 0.2°C month^{-1}.

For March and May, the distributions of various terms are slightly different compared with April. For example, the net surface heat flux dominates the change of SST in almost the whole region in March; in May, the time-varying term is negative in the region from Somalia to the coast of southern India, and the entrainment is the most important process controlling SST in the region southwest of India (Rao and Sivakumar, 1999). However, many features remain the same, for example, in the Arabian Sea and the Bay of Bengal, the time-varying term is positive and the net surface heat flux is the main cause of the increase of SST (figures not shown).

4.2.3 *For July* (*summer*)

For July, the time-varying term (upper left panel of Fig. 8) is negative in the whole region; the contour does not parallel the equator but is roughly along the coast of the Arabian Sea and the Bay of Bengal; the maximum rate of decrease appears near the Somali coast with a value exceeding –2.0°C month^{-1}. South of 10°S, the rate of temperature decrease increases with latitude to value of about −0.6°C month^{-1} near 20°S.

A prominent feature in this month is that the horizontal advection (lower left panel of Fig. 8) plays a major role in the evolution of SST for the large region from 10°S to 10°N west of 90°E, including the Somali and Arabian coast. For the region north of the equator, especially along the Somali coast, horizontal advection leads to SST cooling, whereas for the region between 10°S and the equator, horizontal advection warms SST. The former is closely related to the Somali current, and the latter is due to the influence of the Indonesian throughflow (Masumoto and Yamagata, 1996).

The entrainment (lower right panel of Fig. 8) is dominant along the coast of the Arabian Sea and the west coast of the Bay of Bengal, as well as just south of the equator, west of 90°E, in cooling SST. The net surface heat flux is now the major factor to determine SST for the region south of 10°S, the coast of Sumatra and most of the Bay of Bengal, also causing SST to cool (upper right panel of Fig. 8). It is obvious that

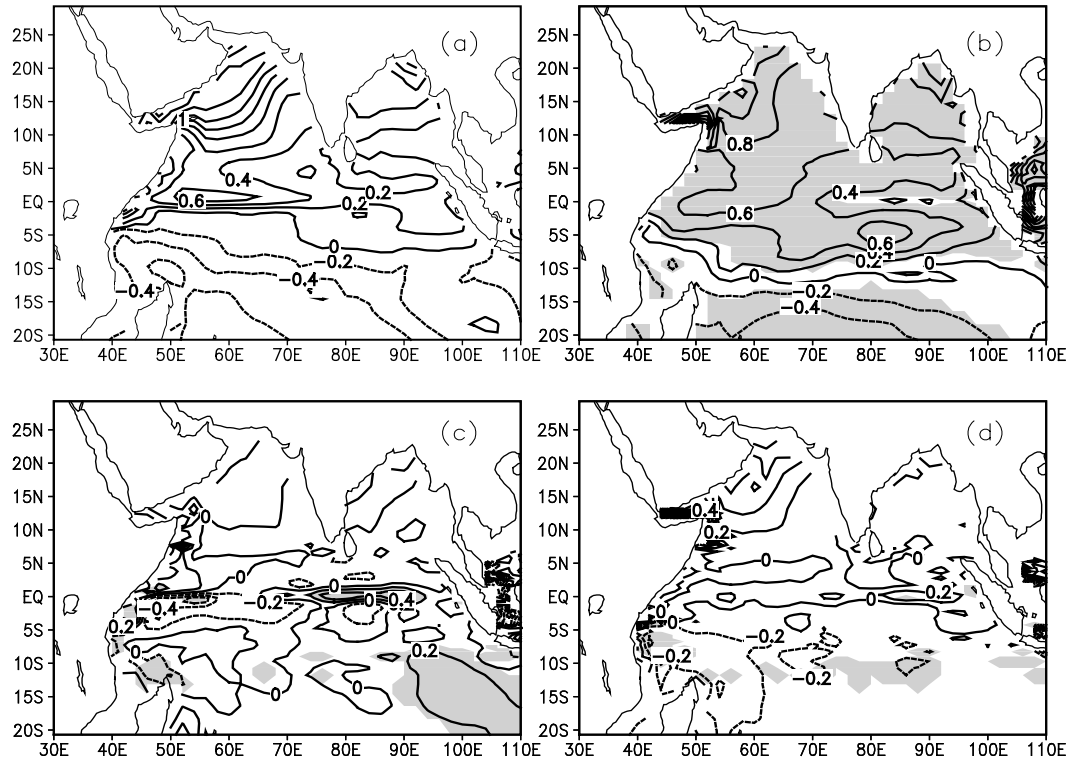

Fig. 7. Same as Fig. 6, but for April. Contour interval: 0.2°C month^{-1}.

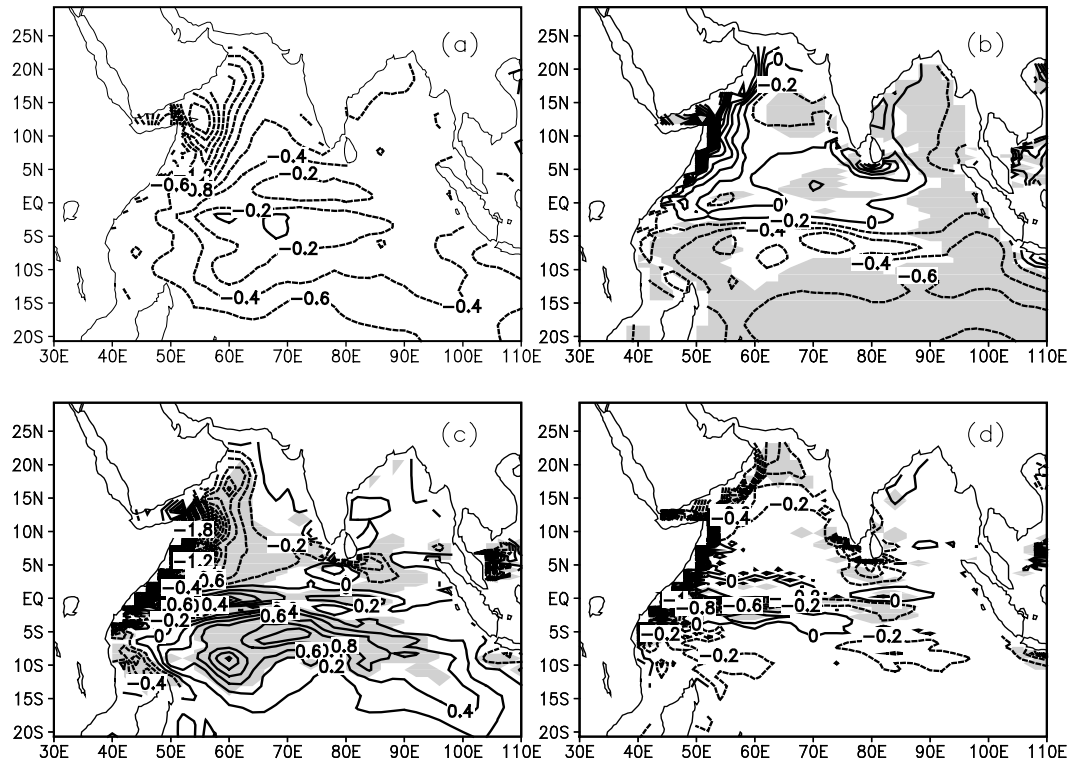

Fig. 8. Same as Fig. 6, but for July. Contour interval: 0.2°C month^{-1}.

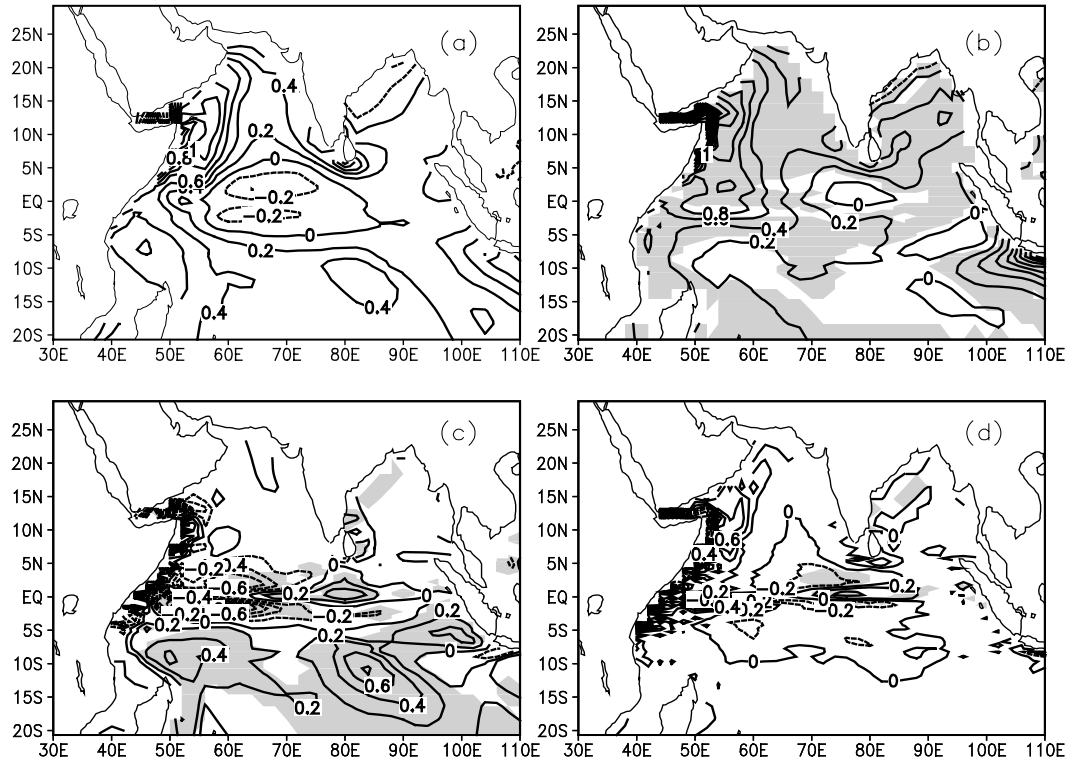

Fig. 9. Same as Fig. 6, but for October. Contour interval: 0.2°C month^{-1}.

these two terms have important effects for the real variability of the SST in this month.

As can be expected, for June and August, the distributions of various terms have some differences compared with those in July. For example, in June, entrainment is the most important process in determining SST change for the central Arabian Sea, rather than horizontal advection as in July; the difference between August and July is relatively small (figures not shown).

4.2.4 *For October* (*autumn*)

In October, the SST increases except in the central equatorial Indian Ocean and the west part of the Bay of Bengal (upper left panel of Fig. 9). For most parts of the region north of the equator, the net surface heat flux is the dominant term in SST change (upper right panel of Fig. 9); whereas for the variation of SST in most parts of the region south of the equator, the horizontal advection is the dominant one (lower left panel of Fig. 9). The role of the entrainment term is very small (lower right panel of Fig. 9).

The patterns of various terms in September are basically the same compared with those in October. In November, the temperature (SST) decreases over most of the Arabian Sea and the whole of the Bay of Bengal; the net surface heat flux is nearly the unique factor that influences SST in this month (figures not shown).

4.3 *Comparison of different regions based on the new Eq. (5)*

Equation (5) can be used to study the dynamics of SST change for any region of interest, not limited to one point, as discussed above. As an illustration, only two regions, namely, north and south of the equator of the tropical Indian Ocean, are analyzed and compared here (Figs. 10 and 11).

4.3.1 *North of the equator*

Figure 10 shows the annual cycle of several terms in Eq. (5), averaged over the region north of the equator of the Indian Ocean. The solid line represents the time-varying term of SST; the dot-and-dash line, dashed line, and dotted line represents the net surface heat flux term, horizontal advection term and entrainment term, respectively. The term across depth h and the term caused directly by horizontal diffusion of $\overline{T}$ are not shown due to their small values and for a clearer plot.

It is evident that the area-mean SST starts to rise from February, and the rate of increase reaches a maximum in April with a value of 0.7°C month^{-1}. After April, the rate of increase drops rapidly. SST begins

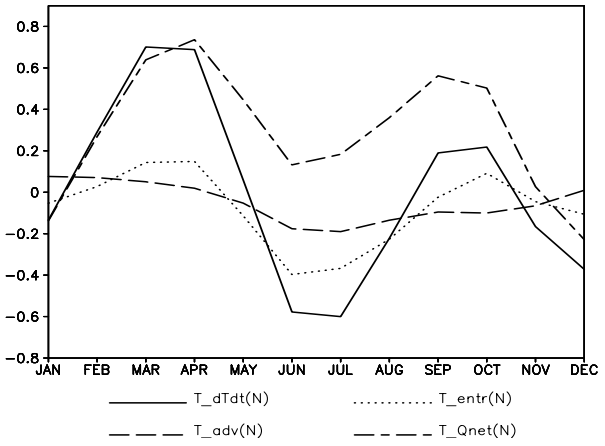

Fig. 10. The annual cycle of various terms, averaged over the region north of the equator of the Indian Ocean. The solid line represents the time-varying term of SST; the dot-and-dash line, dashed line, and dotted line represents the net surface heat flux term, horizontal advection term and entrainment term, respectively; the second and the third terms on the right side of Eq. (5) are not shown due to their small values and for a clearer plot. Units: °C month^{-1}.

to decrease from June with a maximum rate of −0.6°C month^{-1} in July. In September and October, SST rises again with a smaller rate of about 0.2°C month^{-1}. From November to January, SST drops again, but the rate of decrease is smaller than that in summer with a maximum value of less than −0.4°C month^{-1}. This (asymmetrical) semiannual variability of temperature is intimately related to the Indian monsoon.

The net surface heat flux and the entrainment also have semiannual variations with maxima in spring and autumn and minima in winter and summer. Except for December and January, the net surface heat flux warms SST, and the maximal heating rate occurs in April with a value exceeding 0.7°C month^{-1}. The entrainment warms SST in spring and autumn but cools it in winter and summer, and the maximal heating and cooling rates are about 0.15°C month^{-1} and −0.4°C month^{-1}, appearing in spring and summer, respectively. The SST change in this region is mainly determined by the two such processes. The horizontal advection has a cooling rate of about −0.15°C month^{-1} in summer and a smaller heating rate in winter.

These characteristics are basically consistent with those described in section 4.2.

The relationship between the semiannual period of SST in this region and the monsoon activity can be briefly described as follows. In spring, the strong solar radiation associated with less cloud warms the water, leading to the highest SST in the year. After the onset of the Indian summer monsoon, the intense coastal upwelling and offshore advection of cold waters in response to strong monsoon winds drop the temperature drastically. During boreal autumn, the stronger solar radiation warms the water again, leading to the second highest SST. The cold winter monsoon from the Asian continent gives rise to another falling phase of SST. A semiannual period of SST is thus formed in this region.

4.3.2 *South of the equator* (*to* 20°S)

There are quite different features for these terms in this region (Fig. 11) compared with those north of the equator of the Indian Ocean (Fig. 10). The area-mean SST decreases from April to August with a maximal rate of decrease of –0.6°C month^{-1} in June, and increases from October to February with a maximal rate of increase of 0.45°C month^{-1} in December. A prominent period of one year can be seen for this time-varying term. The net surface heat flux also exhibits a period of one year. This period is related to the march of the Sun in one year since the influence of land is smaller in this region. The horizontal advection warms SST throughout one year with a maximal rate of nearly 0.3°C month^{-1} in August. This is related to the influence of the Indonesian throughflow that transports maximum heat from the Pacific to the Indian Ocean in August (Godfrey, 1996). The entrainment cools SST from March to August with a maximal rate of –0.2°C month^{-1} appearing from May to June; it warms SST in other months but the magnitude is smaller. A period of one year is also shown for this term.

These characteristics are also basically consistent with those described in section 4.2.

Obviously, such a method can be applied to other regions of the Indian Ocean. What is more, it can

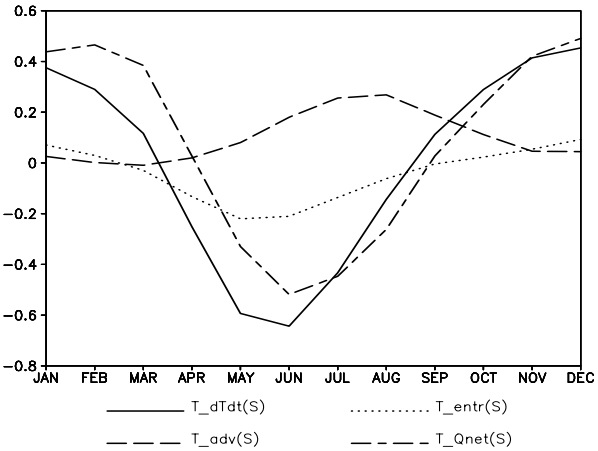

Fig. 11. Same as Fig. 10, but for the region south of the equator (to 20°S). Unit: °C month^{-1}.

also be used to study the mechanism of the interannual variability of SST in various regions of the Indian Ocean. These topics will be described in another paper.

5. Conclusion

SST has a large significance in climate and is determined by many processes. To study the mechanism of SST changes, it is useful to compare the relative importance of different processes in its variation. Based on the output from an ocean general circulation model (MOM2) with a 10-year integration, an attempt is made to this issue. The main results are as follows.

(1) A new equation is derived. This is a general form of an equation for diagnosing SST change "explicitly". All other equations that are widely used in the study of the mechanism of SST (e.g., Steven and Niller, 1983; Feng et al., 1998; Qiu, 2000) are its special case. So this equation is meaningful at least in the qualitative analysis of SST change. In fact, we compared quantitatively the relative role of different processes in determining the seasonal variation of SST for the tropical Indian Ocean.

(2) The net surface heat flux is the most important factor that affects SST over the Arabian Sea, Bay of Bengal and the region south of the equator in January; in April, its influence covers almost the whole region studied; whereas for July and October, this term shows significance mainly in the regions south of 10°S and north of the equator, respectively.

(3) The horizontal advection dominates in the East African-Arabian coast and the region around the equator in January and July, as well as the region south of 10°S in October.

(4) The entrainment is significant only in a narrow band centered on 10°S in April and the coastal region around the Arabian Sea and the equator in July.

(5) The SST decreases in the Arabian Sea and the Bay of Bengal in January and July, and increases in April and October, showing an (asymmetrical) semiannual variability. By contrast, the SST in the region south of the equator has an annual variability, decreasing in April and July and increasing in October and January.

It should be pointed out that only the dynamics of the seasonal cycle of SST are studied in this paper; the following work will mainly focus on the interannual variability of SST in the tropical Indian Ocean. We also need to investigate these issues in detail, using output from ocean models with higher resolution and a longer time integration.

Acknowledgments. The authors would like to thank Y. L. Zhang, A. Schiller and R. Fiedler for their abundant work in ocean modeling. This study was supported by the Key Program of the National Natural Science Foundation of China (NSFC) under Grant No. 40233033.

REFERENCES

Behera, S. K., P. S. Salvekar, and T. Yamagata, 2000: Simulation of interannual SST variability in the tropical Indian Ocean. *J. Climate*, **13**, 3487–3499.

Carton, J. A., G. Chepurin, and X. Cao, 2000: A simple ocean data assimilation analysis of the global upper ocean 1950–95, Part II: Results. *J. Phys. Oceanogr.*, **30**, 311–326.

Chen, D., L. M. Rothstein, and A. J. Busalacchi, 1994: A hybrid vertical mixed-layer scheme and its application to tropical ocean models. *J. Phys. Oceanogr.*, **24**, 2156–2179.

Chen Lieting, 1991: Effect on zonal difference of sea surface temperature anomalies in the Arabian Sea and the South China Sea on summer rainfall over the Yangtze River. *Scientia Atmospheric Sinica*, **15**(1), 33–42. (in Chinese)

Feng, M., P. Hacker, and R. Lukas, 1998: Upper ocean heat and salt balances in response to a westerly wind burst in the western equatorial Pacific during TOGA COARE. *J. Geophys. Res.*, **103**, 10289–10311.

Ffield, A., and A. L. Gordon, 1992: Vertical mixing in the Indonesian thermocline. *J. Phys. Oceanogr.*, **22**, 184–195.

Godfrey, J. S., 1996: The effect of the Indonesian Throughflow on ocean circulation and heat exchange with the atmosphere: A review. *J. Geophys. Res.*, **101**(C5), 12217–12237.

Godfrey, J. S., and A. Schiller, 1997: Tests of mixed-layer schemes and surface boundary conditions in an Ocean General Circulation Model, using the IMET data set. CSIRO Marine Laboratories Report, 321pp.

Hellerman, S., and M. Rosenstein, 1983: Normal monthly wind stress over the world ocean with error estimates. *J. Phys.Oceanogr.* **13**, 1093–1104.

Hu Ruijin, 2003: Study on the heat budget and the meridional circulation of the tropical Indian Ocean. Ph. D. dissertation, Ocean University of China, 99pp. (in Chinese)

Legler, D. M., I. M. Navon, and J. J. O'Brien, 1989: Objective analysis of pseudostress over the Indian Ocean using a direct-minimization approach. *Mon. Wea. Rev.*, **117**, 709–720.

Levitus, S., R. Burgett, and T. P. Boyer, 1994: World Ocean Atlas 1994, Volume 3: Salinity. *NOAA Atlas NESDIS 3*, U.S. Department of Commerce, Washington D. C., 99pp.

Li Chongyin, and Mu Mingquan, 2001: The dipole in the equatorial Indian Ocean and its impacts on climate. *Chinese J. Atmos. Sci.*, **25**(4), 433–443. (in Chinese)

Liu Hailong, Zhang Xuehong, and Li Wei, 2001: The heat balance in the western equatorial Pacific warm pool during the westerly wind bursts: A case study. *Adv. Atmos. Sci.*, **18**(5), 882–896. (in Chinese)

Masumoto, Y., and T. Yamagata, 1996: Seasonal variations of the Indonesian Throughflow in a general circulation model. *J. Geophys. Res.*, **101**, 12287–12293.

McCreary, J. P., P. K. Kundu, and R. L. Molinari, 1993: A numerical investigation of dynamics, thermodynamics and mixed-layer processes in the Indian Ocean. *Progress in Oceanography*, **31**, 181–244.

McPhaden, M. J., 1982: Variability in the central Indian Ocean, II: Oceanic heat and turbulent energy balances. *J. Mar. Res.*, **40**, 403–419.

McPhaden, M. J., and S. P. Hayes, 1991: On the variability of winds, sea surface temperature, and surface layer heat content in the western equatorial Pacific. *J. Geophys. Res.*, **96**(suppl.), 3331–3342.

Murtugudde, R., and A. J. Busalacchi, 1999: Interannual variability of the dynamics and thermodynamics of the tropical Indian Ocean. *J. Climate*, **12**, 2300–2326.

Nicholls, N., 1985: Sea surface temperature and Australia winter rainfall. *J. Climate*, **2**, 965–973.

Pacanowski, R. C., 1995: MOM2 Documentation User's Guide and Reference Manual, Version 1.0. GFDL Ocean Technical Rep. 3, 232pp.

Qiu, B., 2000: Interannual variability of the Kuroshio Extension system and its impact on the wintertime SST field. *J. Phys. Oceanogr.*, **30**, 1486–1502.

Qu, T., G. Meyers, and J. S. Godfrey, 1994: Ocean dynamics in the region between Australia and Indonesian and its influence on the variation of sea surface temperature in a global general circulation model. *J. Geophys. Res.*, **99**, 18433–18445.

Rao, R. R., and R. Sivakumar, 1999: On the possible mechanisms of the evolution of a mini-warm pool during the presummer monsoon season and the genesis of onset vortex in the southeastern Arabian Sea. *Quart. J. Roy. Meteor. Soc.*, **125**, 787–809.

Rao, R. R., and R. Sivakumar, 2000: Seasonal variability of near-surface thermal structure and heat budget of the mixed layer of the tropical Indian Ocean from a new global ocean temperature climatology. *J. Geophys. Res.*, **105**, 995–1015.

Saji, N. H., B. N. Goswami, P. N. Vinayachandran, and T. Yamagata, 1999: A dipole in the tropical Indian Ocean. *Nature*, **401**, 360–363.

Schiller, A., J. S. Godfrey, P. C. McIntosh, G. Meyers, and S. E. Wijffels, 1998: Seasonal near-surface dynamics and thermodynamics of the Indian Ocean and the Indonesian Throughflow in a global ocean general circulation model. *J. Phys. Oceanogr.*, **28**, 2288–2312.

Schott, F. A., and P. M. Jr. McCreary, 2001: The monsoon circulation of the Indian Ocean. *Progress in Oceanography.*, **51**, 1–123.

Shetye, S., 1986: A model study of the Arabian Sea temperature. *J. Mar. Res.*, **44**, 521–542.

Shukla, J., and D. A. Mooley, 1987: Empirical prediction of the summer monsoon rainfall over India. *Mon. Wea. Rev.*, **115**, 695–703.

Simonot, J. Y., and H. L. Letreut, 1986: A climatological field of mean optical properties of the world ocean. *J. Geophys. Res.*, **91**, 6642–6646.

Stevenson, J. W., and P. P. Niiler, 1983: Upper ocean heat budget during the Hawaii-to-Tahiti shuttle experiment. *J. Phys. Oceanogr.*, **13**, 1894–1907.

Stricherz, J., J. J. O'Brien, and D. Legler, 1992: *Atlas of Florida State University Tropical Pacific Winds for TOGA 1966–1985*. The Florida State University, 256pp.

Webster, P. J., A. M. Moore, J. P. Loschnigg, and R. R. Leben, 1999: Coupled ocean-atmosphere dynamics in the Indian Ocean during 1997–98. *Nature*, **401**, 356–359.

Wu Guoxiong, Liu Ping, Liu Yimin, and Li Jianping, 2000: Impacts of the sea surface temperature anomaly in the Indian Ocean on the subtropical anticyclone over the western Pacific—Two-stage thermal adaptation in the atmosphere. *Acta Meteorologica Sinica*, **58**(5), 513–522. (in Chinese)

Xiao Ziniu, and Yan Hengming, 2001: A numerical simulation of the Indian Ocean SSTA influence on the early summer precipitation of the Southern China during an El Nino year. *Chinese J. Atmos. Sci.*, **25**(2), 173–183. (in Chinese)